PLASTIC UPCYCLING

Hydroformylation of pyrolysis oils to aldehydes and alcohols from polyolefin waste

Houqian Li[1], Jiayang Wu[1], Zhen Jiang[1], Jiaze Ma[1], Victor M. Zavala[1,2], Clark R. Landis[3], Manos Mavrikakis[1], George W. Huber[1]*

Waste plastics are an abundant feedstock for the production of renewable chemicals. Pyrolysis of waste plastics produces pyrolysis oils with high concentrations of olefins (>50 weight %). The traditional petrochemical industry uses several energy-intensive steps to produce olefins from fossil feedstocks such as naphtha, natural gas, and crude oil. In this work, we demonstrate that pyrolysis oil can be used to produce aldehydes through hydroformylation, taking advantage of the olefin functionality. These aldehydes can then be reduced to mono- and dialcohols, oxidized to mono- and dicarboxylic acids, or aminated to mono- and diamines by using homogeneous and heterogeneous catalysis. This route produces high-value oxygenated chemicals from low-value postconsumer recycled polyethylene. We project that the chemicals produced by this route could lower greenhouse gas emissions ~60% compared with their production through petroleum feedstocks.

Olefins are a central building block of modern chemicals and polymers (*1*). Polyolefins, polyesters, surfactants, alcohols, amines, and carboxylic acids all are manufactured from olefins (*2*). Natural petroleum products, such as crude oil, natural gas, and naphtha, have low concentrations (3 wt %) of olefins (Fig. 1). A variety of energy-intensive chemical steps, such as steam cracking, are used to produce olefins from petroleum. More sustainable means for olefin production and use are desirable, for example, recovering olefins from waste plastics followed by upgrading the olefins. Here, we demonstrate how waste plastics can be converted into olefins by thermal depolymerization reactions such as pyrolysis. These olefins can then undergo hydroformylation and further hydrogenation to produce mono- and dialcohols. Specifically, we showcase a route to produce functional chemicals from postconsumer recycled (PCR) waste plastics collected from an operational material recovery facility using a combination of thermal depolymerization to produce an olefin-rich pyrolysis oil; homogeneous hydroformylation catalysis to transform a complex mixture of mono-olefins and diolefins in the pyrolysis oil into aldehydes; and heterogeneous catalysis to reduce, oxidize, or aminate the aldehydes. We also demonstrate a separation scheme to produce high-purity diolefins and mono-olefins that would be acceptable for polymer-grade applications.

Pyrolysis of polyolefins produces high concentrations (~50 wt %) of olefins (Fig. 1). Four different plastics were pyrolyzed in a fluidized bed reactor at a temperature of 500°C and a residence time of 20 s, which included PCR high-density polyethylene (HDPE), virgin HDPE, virgin polypropylene (PP), and virgin low-density polyethylene (LDPE), and generated pyrolysis oil with varied compositions (fig. S2A). The liquid product yields (pyrolysis oil) were >60 wt % for all of these plastics, with the remainder of the products being gas and char (details in table S1). For simplicity in our analytical work, the pyrolysis oil was distilled to light and heavy cut (details in supplementary materials). More than a thousand compounds (>1000 blobs in gas chromatogram) were identified in the whole pyrolysis oils depicted in Fig. 2A and fig. S5A. The zoomed-in chromatogram region in this figure shows a more detailed distribution of product classes. The light cut was analyzed by detailed hydrocarbon analysis, the heavy cut was analyzed by nitric oxide ionization spectroscopy evaluation, and both cuts were analyzed by gas chromatography measurements (details in supplementary materials), which confirmed that the pyrolysis oil is composed of mono-olefins (34 to 50 wt %), paraffins (20 to 39 wt %), monoaromatics (11 to 23 wt %), diolefins (6 to 13 wt %), and dicycloaromatics (<5 wt %) that ranged from C5 to C40 (fig. S3). These results agree with the literature reported values with 40 to 70 wt % of mono-olefins, 8 to 40 wt % paraffins, 4 to 13 wt % of monoaromatics, and 5 to 20 wt % of diolefins (*3*–*6*). The structure of these products changes depending on the type of polyolefin that is used. For example, HDPE products are highly linear, whereas LDPE products are more branched. Thermal depolymerization, by pyrolysis or liquefaction, of waste plastics is currently receiving tremendous industrial interest with >10 companies having made recent announcements on building commercial facilities (*7*–*11*). For example, Dow Inc. recently announced the construction of the world's largest plastic depolymerization plant [120 kilo–metric tons (kton)/year] in Europe (*12*). These companies primarily use pyrolysis oils as feedstocks to replace naphtha in petroleum refineries or steam cracking (*13*). These approaches typically require hydrotreating of the pyrolysis oil and do not take advantage of the olefin functionality. It has been estimated that the overall yield of polyolefins from this route is <30 wt % of the virgin plastic (*10*, *13*).

Hydroformylation of pyrolysis oil followed by hydrogenation

A commercial $Co_2(CO)_8$ catalyst was modified with or without phosphine ligands [2-bis (diphenylphosphino) ethane monoxide and tri-*n*-butylphosphine] for the hydroformylation of hexenes and hexadienes to establish appropriate reaction conditions. Low aldehyde yields (<40%) were obtained when ligands were used (table S2). Near-complete conversion of hexene was obtained with unmodified $Co_2(CO)_8$, which is consistent with Zhang and co-workers' recent report (*14*). Hydroformylation of 1-hexene, *cis*-2-hexene, and 1,5-hexadiene produced the respective aldehydes in near-quantitative yields under these same conditions, as shown in table S2. A high heptanal selectivity (>80%) was observed for the hydroformylation of both 1-hexene and *cis*-2-hexene (fig. S4), which suggests that the internal olefins can also be converted into terminal aldehydes under this reaction condition. As shown in Fig. 2B, hydroformylation of pyrolysis oils under the same reaction condition produced up to 60 wt % yield of the aldehydes from the pyrolysis oil without a solvent (Fig. 3). Recent studies have demonstrated that heterogeneous catalysts can also be used for hydroformylation (*15*–*18*). Hydroformylation of the light cut (table S3) of the pyrolysis oil was performed separately from that of the heavy cut (table S4), and the products were characterized by two-dimensional (2D) gas chromatography (GC × GC), 1D/2D nuclear magnetic resonance (NMR), and CHN(O)S elemental analysis.

The formation of aldehydes from pyrolysis oil (light cut) was evidenced by the appearance of features in the region characteristic of alcohols and aldehydes in GC × GC chromatogram as exhibited in the inset of Fig. 2B. Compared with Fig. 2A, changes in the positions of the features in the second dimension (^{2}D) retention time are observed in Fig. 2B, which indicates that the hydroformylation changed the polarity of the pyrolysis oil. Minor changes in the positions of the features in first dimension (^{1}D) retention time suggest that the carbon number changed slightly after the hydroformylation process. More than 90% of the olefins in the pyrolysis oil were converted into aldehydes, as can be calculated by subtracting the volume of the features in Fig. 2A from that in Fig. 2B (table S2; see supplementary materials). A similar performance was observed in the hydroformylation of the pyrolysis oil heavy cut (table S2 and

[1]Department of Chemical and Biological Engineering, University of Wisconsin–Madison, Madison, WI 53706, USA. [2]Mathematics and Computer Science Division, Argonne National Laboratory, Lemont, IL 60439, USA. [3]Department of Chemistry, University of Wisconsin–Madison, Madison, WI 53706, USA.
*Corresponding author. Email: gwhuber@wisc.edu

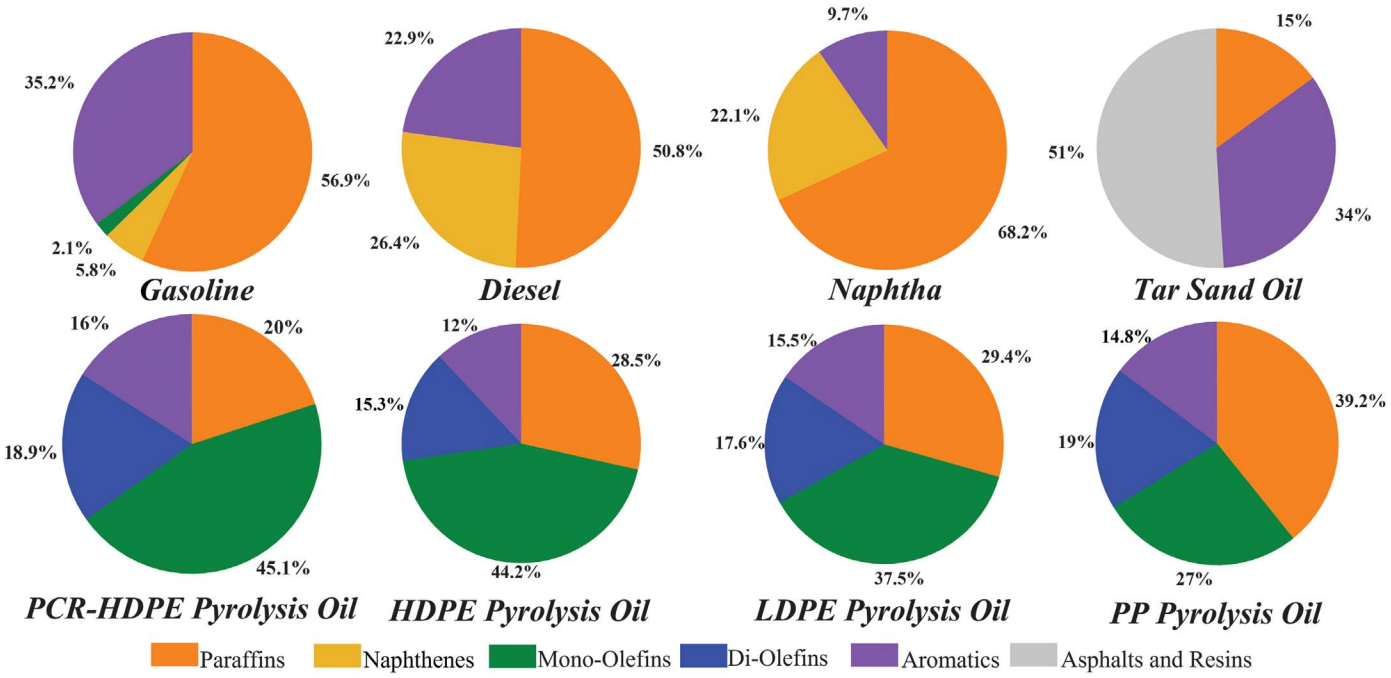

Fig. 1. Chemical composition of petroleum products and plastic oils derived from pyrolysis of PCR HDPE, HDPE, LDPE, and PP conducted in this work. Compositions of gasoline, diesel, naphtha, and tar sand oil are obtained elsewhere (*48*, *49*). See supplementary materials for detailed pyrolysis experiments.

fig. S5). The formation of aldehydes was further supported by ^{13}C-NMR analysis as depicted in Fig. 2E (full spectrum in fig. S6). Simultaneous decrease in peaks in the C=C region [105 to 150 parts per million (ppm)] and appearance of the peaks in the 200- to 210-ppm region indicates the formation of C=O groups after hydroformylation. The ^{1}H-^{13}C heteronuclear single quantum coherence (HSQC) spectrum of the upgraded oil after hydroformylation confirms the formation of the aldehydes (fig. S7). Peaks in the 55- to 70-ppm region of Fig. 2E indicate alcohol formation. The oxygen content in the hydroformylation products was further confirmed by CHN(O)S elemental analysis as 14 and 5 wt % oxygen in the light and heavy cut of the oil, respectively. Pyrolysis oils generated from waste plastics can contain a number of other elements in both organic and inorganic forms, including N, O, Cl, Fe, Si, K, Ca, S, Zn, Cu, Ti, and Al (*10*). Catalytic hydroformylation is tolerant of several of these contaminants, which include carbonyls, ethers, alcohols, carboxamides, amines, silanes, siloxanes, halide salts, and iron impurities (*19*–*23*). Vinyl/allyl halides and conjugated diolefins (*24*) are expected to be catalyst poisons during hydroformylation and can be removed by pretreating waste plastics before pyrolysis or adjusting parameters in the plastic pyrolysis.

Catalytic hydrogenation of the hydroformylated pyrolysis oils by using varied metal catalysts, after removal of the Co catalyst (table S5), yields alcohols. The shifting of the GC × GC features to longer ^{1}D retention time (Fig. 2C) implies that the aldehydes in the "hydroformylated pyrolysis oil" light cut were converted to alcohols because the alcohols have large ^{1}D retention time compared with the same carbon number aldehydes (fig. S8). Standard ^{1}H NMR and quantitative ^{13}C NMR were used to estimate the aldehyde conversion in the "hydroformylated pyrolysis oil" (figs. S6 and S7). The hydrogenation of the "hydroformylated pyrolysis oil" was also conducted in a fixed bed reactor with 20% Ni/SiO_2, with >90% of the aldehydes being reduced to the alcohols for both the light and heavy cut as shown in table S5 and in Fig. 2F. The peaks in the C=O region disappeared, and peaks in the C-OH region appeared. Most of the alcohols are primary alcohols as evidenced by the ^{1}H-^{13}C HSQC spectrum (light cut in Fig. 2G, heavy cut in fig. S7).

Input–output analysis

The overall mass balances of products from PCR colored HDPE are plotted as a Sankey diagram in Fig. 3. Pyrolysis of PCR HDPE generates pyrolysis oil, which undergoes hydroformylation and hydrogenation that produces primarily paraffins, aromatics, monoalcohols, and dialcohols in the range of C5 to C20. For example, pyrolysis of 100 kg of HDPE would generate 80 kg of plastic oil that contained 51 kg of olefins. The olefins then undergo hydroformylation to form aldehydes, which are subsequently hydrogenated into alcohols that generate 49 kg of monoalcohols and 13 kg of diols in the final product (assuming a 100-kg HDPE feed input). The synthesis gas (CO + H_2) and hydrogen required for this conversion could be produced from biomass, which further lowers the process carbon and energy input (*25*). The monoaromatics, C5 to C8 paraffins, and >C8 hydrocarbons (paraffins and multicyclic aromatics) can be used for polyethylene terephthalate (PET) and polystyrene (PS) manufacture, gasoline, and diesel, respectively, at $600 to $800 per ton (*26*). The C6 to C12 alcohols (0.42 tons per ton of HDPE) can be sold as plasticizers, which sell for $1600 to $2300 per ton (*27*). The >C12 alcohols (0.07 tons per ton of HDPE) can be used as surfactants and sold for >$2000 per ton (*27*). The diols (0.13 tons per ton of HDPE) are the most valuable product and sell for $3000 to $5000 per ton and can be used to produce polyesters and polyurethanes (*27*).

Theoretical simulations

The ratio of diols to monoalcohols produced by the hydroformylation/hydrogenation process is determined by the diene:mono-olefin ratio in the pyrolysis oil. The hydroformylated products could alternatively be oxidized to carboxylic acids, aminated to amines, or condensed into larger aldehydes. In all cases, the difunctional compound is more valuable than the monofunctional compound; hence, it would be desirable to tune the pyrolysis to produce more dienes. Previous work modeling pyrolysis has been focused on the development of

kinetic models with limited attention to molecular scale bond-breaking or –making events (*8*, *28*). Accordingly, we performed an ab initio investigation of the thermal depolymerization chemistry that leads to the formation of monoolefins, paraffins, and dienes in the pyrolysis oils using the second Møller–Plesset perturbation theory (*29*) and 6-31++G** basis sets (*30*, *31*) in the *Gaussian 09* package (computational details in supplementary materials). The minimum energy path for the thermal decomposition of HDPE (modeled by decane) is initiated by backbone C-C bond breaking with a transition state (TS) energy of G^* = 352.9 kJ/mol, which leads to the formation of two radicals ($\bullet C_5H_{11}$) (intermediate 1) (Fig. 4A). That step is followed by a H abstraction step that proceeds from a middle $-CH_2-$ site of one radical

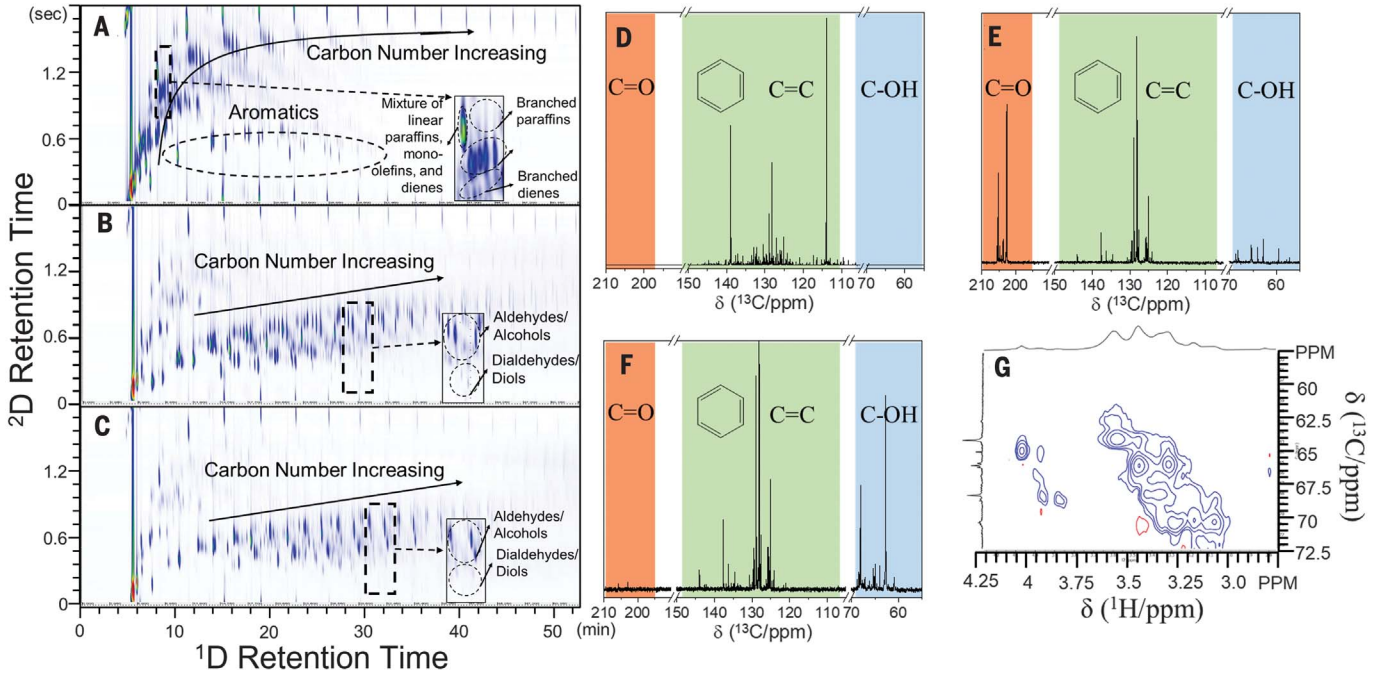

Fig. 2. Hydroformylation of pyrolysis oil (light cut) catalyzed by $Co_2(CO)_8$ and hydrogenation of the "hydroformylated oil" catalyzed by 20% Ni/SiO_2. (**A**) GC × GC analysis of HDPE pyrolysis oil light cut. (**B**) GC × GC analysis of the oil after hydroformylation catalyzed by $Co_2(CO)_8$ in a 350-ml stainless steel batch reactor for 3 hours. Conditions: 120°C, 70 bar synthesis gas (CO/H_2 = 1), 900 rpm, 10 wt % $Co_2(CO)_8$ in oil. (**C**) GC × GC analysis of the hydroformylated oil after hydrogenation catalyzed by 20%Ni/SiO_2 in a continuous flow reactor for 5 hours. Conditions: 100°C, 78 bar H_2, weight hourly space velocity 1 $hour^{-1}$. Insets in (A) to (C) represent magnified boxed region. The species concentration increases from blue to green. (**D**) ^{13}C NMR spectra of HDPE pyrolysis oil light cut. (**E**) ^{13}C NMR spectra of hydroformylated oil. (**F**) ^{13}C NMR spectra of hydroformylated oil after hydrogenation. (**G**) ^{1}H-^{13}C HSQC NMR spectrum of hydroformylated oil after hydrogenation. Blue and red represent primary and secondary carbons, respectively.

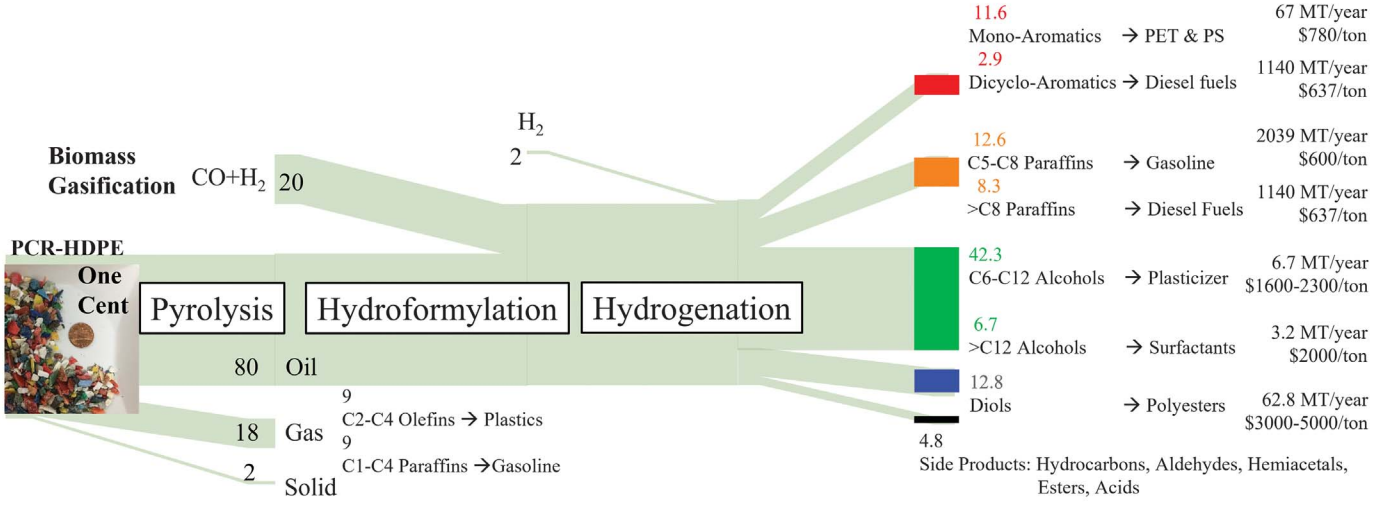

Fig. 3. Input–output analysis, global production, and market price for the production of aromatics, paraffins, monoalcohols, and dialcohols from waste plastics. Mass balance in the pyrolysis, hydroformylation, and hydrogenation steps are in the range of 100 ± 15%. MT, million metric tons.

(identified as the most feasible site for H transfer; details in fig. S11) to the other radical (terminal .CH_2- site) characterized by an activation Gibbs free energy barrier of ΔG^* = 119.4 kJ/mol. This step leads to the formation of pentane (C_5H_{12}) and a metastable C_5H_{10} structure that contains a triangular C-ring (intermediate 2). Lastly, 326.3 kJ/mol is required to open the triangular C-ring, which leads to the final pyrolysis products of pentane and internal pentene (C_5H_{12} and C_5H_{10}, respectively). The overall reaction is exergonic by −48.8 kJ/mol. Three additional reaction paths initiated by H transfer along the HDPE backbone (without radical formation) were also studied, but they are all less favorable than the free-radical path (Fig. 4) already discussed because of the much higher TS energies (G^* = 468.1, 474.5, or 690.6 kJ/mol) (fig. S10). Then, we turned our attention to the diene formation mechanism. First, we determined that the internal conjugated C_7H_{12} is the most stable of the nine linear isomers considered (fig. S12). The most exergonic path (P1, among three possible paths shown in fig. S13) is provided in Fig. 4B with the associated TS energetics. From decane to heptadiene, two consecutive backbone C-C bond-breaking steps and H transfers were needed with mono-olefin as intermediate and paraffins (CH_4 and C_2H_6) as byproducts without hydrogen evolution. This is in good agreement with our experimental findings of <1 wt % yield of H_2 product in both HDPE and LDPE pyrolysis oil (table S7). Along this path, the highest TS energy (G^* = 364.4 kJ/mol) is higher than that (G^* = 352.9 kJ/mol) for the formation of pentane (C_5H_{12}) and internal pentene (C_5H_{10}) discussed above. This TS energy difference leads to a reaction rate for diene production that is lower than the production rate of paraffin plus olefin by a little less than one order of magnitude at 500°C, an estimate that is in near-quantitative agreement with our experimental product distribution (fig. S3). The other two pathways studied for diene (C_7H_{12}) formation (P2 and P3; see details in fig. S13) were both found to be thermodynamically unfavorable compared with P1. We envision that using suitable catalysts to facilitate the radical formation and H abstraction can further enhance selectivity of the pyrolysis process toward production of olefins and diolefins.

Technoeconomic modeling and life cycle assessment

We then developed a process model for producing monoalcohols and diols from the pyrolysis oils with hydroformylation technology (fig. S15 and tables S8 to S10) and used this to estimate the economics and environmental impacts. We considered two different approaches to separate our products as shown in Fig. 5, A and B. Distillation of the hydrogenated products (as shown in Fig. 5A) produces mixtures of monoalcohols, diols, benzene, toluene, and xylenes (BTX), and paraffins. High-purity diols are not attainable if this separation scheme uses only distillation after hydroformylation (details in supplementary materials). However, high-purity diols with <500 ppm of monoalcohols

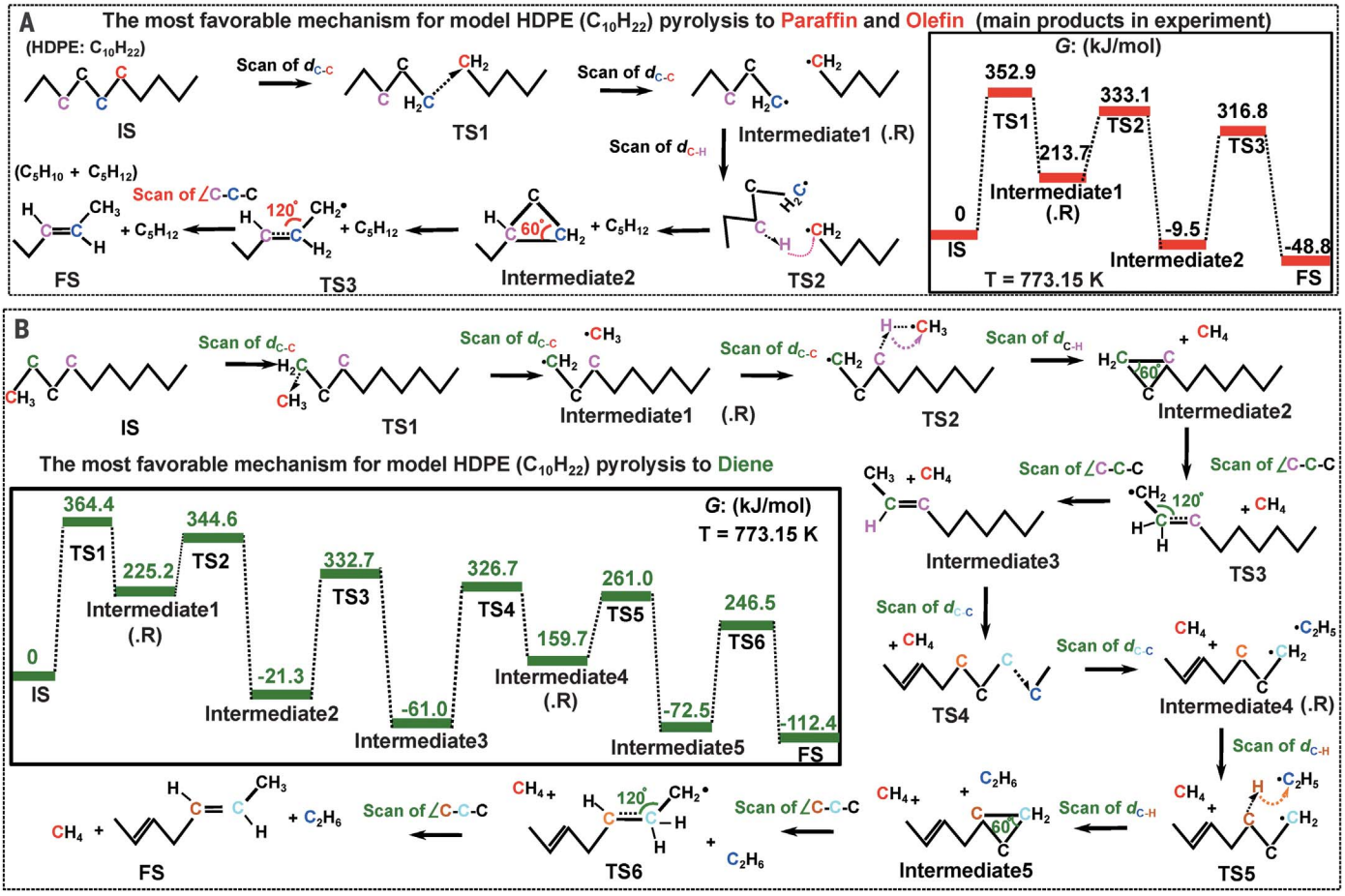

Fig. 4. Mechanistic simulations. (**A** and **B**) The thermodynamically and kinetically most favorable mechanisms for the formation of paraffin and mono-olefin (A) and diolefin (B). Linear decane ($C_{10}H_{22}$) was used as a surrogate molecule for HDPE and its pyrolysis to pentane (C_5H_{12}), pentene (C_5H_{10}), and heptadiene (C_7H_{12}) because of their largest concentrations in each product category according to our experimental results in fig. S3. For comparison, the less favorable mechanisms for the formation of paraffin, mono-olefin, and diolefin are shown in figs. S10, S11, and S14. The simulation temperature (773.15 K = 500°C) is the temperature at which the pyrolysis experiments were performed. FS, final state; IS, initial state.

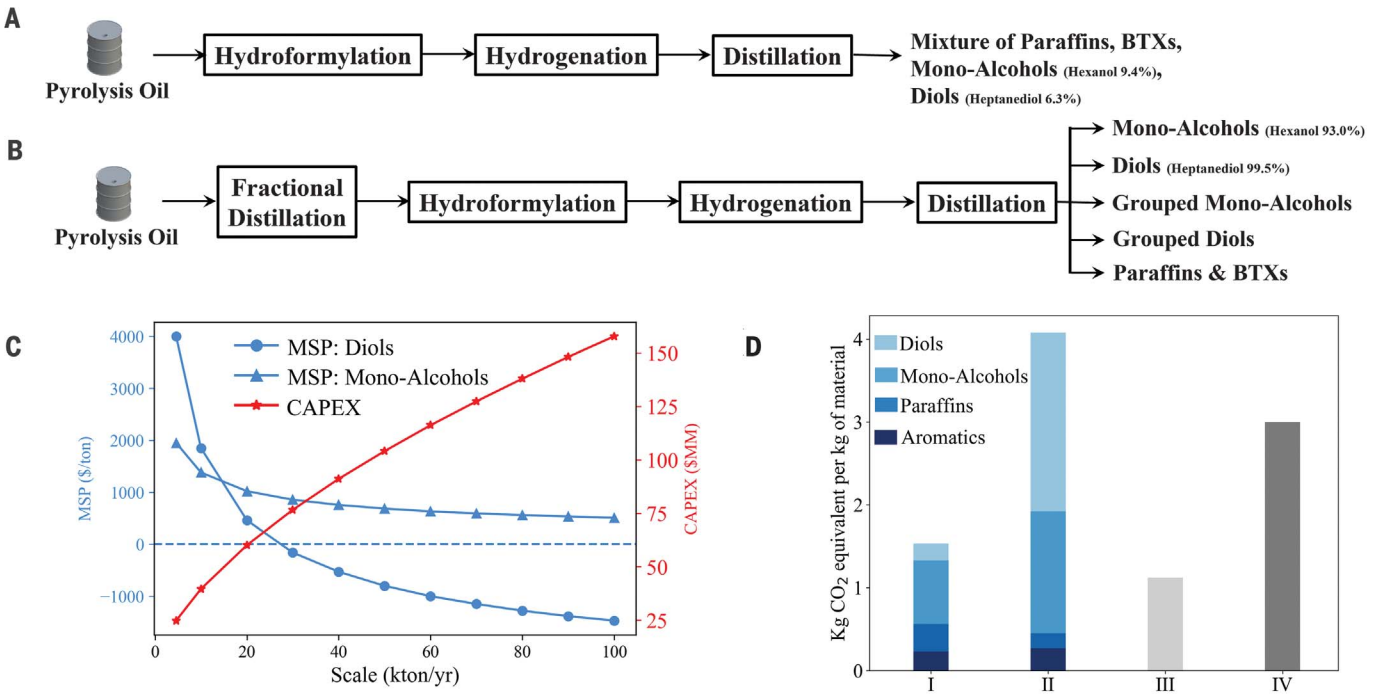

Fig. 5. Technoeconomics. (**A**) Process without pretreatment of pyrolysis oil before hydroformylation. (**B**) Process includes the pyrolysis oil pretreatment into different cuts, followed by hydroformylation, hydrogenation, and separation of each cut. (**C**) Capital expenditure (CAPEX) and MSP of products. (**D**) GHGs from (I) the proposed technology for converting 1 kg of plastic into chemicals, (II) conventional technologies for producing the same amount of chemicals, (III) converting 1 kg of plastic to olefins through pyrolysis and steam cracking, and (IV) incinerating 1 kg of plastic. Details of GHGs are provided in the supplementary materials.

can be produced by fractional distillation of the pyrolysis oil into different fractions, followed by hydroformylation and hydrogenation of each cut, as shown in Fig. 5B. Further separation leads to high-purity monoalcohols (e.g., hexanol 91%) or diols (e.g., heptanediol 99.5%) as an individual component (Fig. 5B and tables S9 and S10). Thus, we show how polymer-grade diols can be produced with a proper separation scheme. The economic potential of the proposed technology is largely influenced by the selling prices of monoalcohol and diol because these products account for >80% of revenue. Accordingly, a sensitivity analysis was conducted to determine the minimum selling prices (MSPs) of monoalcohols and diols under various processing capacities. The MSPs for alcohols equal current market prices ($4000 per and $1950/ton for diols and monoalcohols, respectively) when the plant capacity is set at 4600 tons of plastic per year (Fig. 5C). Because of economies of scale, increasing the plant capacity from 4600 to 16,000 tons per year results in a twofold increase in capital costs, whereas the MSPs for monoalcohol and diol decrease by >50% (compared with market prices). When the production scale reaches 24,000 tons per year, the MSP of diol goes to zero. This suggests that the proposed technology could be economically viable even without revenue from diol at this production level. When setting the production scale to 100,000 tons per year, which is similar to the production scale of a typical chemical plant, the MSPs of two critical products, alcohols and dialcohols, are $508 per ton and −$1470 per ton, respectively. The negative MSP of dialcohols implies that the revenue from other products can not only cover the cost but also generate a profitable stream. Moreover, at this level of production, the annual net profit can amount to as much as $100 million, with a relatively short payback period of 3 years.

The greenhouse gas emissions (GHGs) from recycling 1 kg of plastic waste by using this technology are 1.6 kg CO_2 equiv (tables S11 to S13 and fig. S17), which is ~50% lower than that of incinerating 1 kg of plastic waste (Fig. 5D, I versus IV). Other plastic upcycling strategies, such as producing olefins from plastic pyrolysis oil by using steam cracking, emit ~1.2 kg CO_2 equiv (*13*) per kilogram of plastic processed (fig. S17). The carbon footprint of the proposed technology in this work is comparable with that of the plastic-to-olefin route. GHGs of each grouped species in the final product were calculated by multiplying the total GHGs of this technology by the weight percentage of the specific grouped species. As shown in Fig. 5D, I and II, the diol production route is associated with 0.20 kg CO_2 equiv per 0.14 kg dialcohol produced from 1 kg plastic (or 1.4 kg CO_2 equiv per kilogram of diols). Producing the same diol conventionally from petroleum has >10 times higher emissions [15.1 kg of CO_2 equiv per kilogram of diols (*32*)]. Compared with producing the same amount of chemicals via the traditional route from fossil feedstocks, the proposed technology results in 60% lower GHGs (Fig. 5D, I versus II).

The approach outlined here demonstrates a platform technology for upcycling of waste plastic oils by hydroformylation chemistry. ExxonMobil has filed a patent application for the production of monoalcohols from plastic pyrolysis oils by using hydroformylation and noncatalytic reduction of aldehydes to alcohols with sodium borohydride (*33*). However, a detailed characterization of the reaction chemistry, the product analysis, the economics of the technology, and the environmental impacts are not reported in the patent application. Additionally, the ExxonMobil route did not produce dialcohols. In this study, we elucidated the mechanisms for thermal depolymerization of polyolefin, which provides insights in tuning plastic oil distribution. The aldehydes produced from hydroformylation can be used to produce a range of chemicals that include alcohols, carboxylic acids, and amines. The separation process produces high-purity diols and monoalcohols that are suitable for polymer applications. The olefins in the pyrolysis oil can also undergo hydroaminoalkylation, which generates amines in a single step (*34*–*36*). The branching in the

products can be controlled by tuning the plastic feedstocks. For example, HDPE produces straight-chain products, whereas PP and LDPE create different types of branching in the products (details in figs. S20 and S21 and table S14). Many approaches have been developed to recycle or upcycle waste plastics into varied products, which include hydrogenolysis (*37*, *38*) and catalytic deconstruction (paraffins, olefins, and aromatics) (*39*–*41*), dissolution-based approaches (plastic resins with virgin properties) (*42*), functionalization (plastics with new properties) (*43*), and oxidation (oxygenates) (*44*, *45*). Compared with these routes, the key benefits of the approach reported are production of high-value (>$1600 per ton) monoaldehydes, dialdehydes, monoalcohols, and dialcohols (*46*, *47*), which can be done by using existing hydroformylation infrastructure.

REFERENCES AND NOTES

1. I. Amghizar, L. A. Vandewalle, K. M. Van Geem, G. B. Marin, *Engineering* **3**, 171–178 (2017).
2. Nexant, Independent Market Report on the Global and Indonesian Petrochemicals Industry (2011); https://www.scribd.com/document/217378314/201105151926340-Nexant-Industry-Report-2011 [accessed 2 October 2022].
3. M. Kusenberg *et al*., *Fuel Process. Technol.* **227**, 107090 (2022).
4. A. Gala, M. Guerrero, B. Guirao, M. E. Domine, J. M. Serra, *Energy Fuels* **34**, 5969–5982 (2020).
5. Y. Zhang *et al*., *ACS Sustain. Chem. Eng.* **10**, 91–103 (2022).
6. D. Zhao, X. Wang, J. B. Miller, G. W. Huber, *ChemSusChem* **13**, 1764–1774 (2020).
7. H. Li *et al*., *Green Chem.* **24**, 8899–9002 (2022).
8. O. Dogu *et al*., *Prog. Energy Combust. Sci.* **84**, 100901 (2021).
9. A. Eschenbacher *et al*., *Appl. Catal. B* **309**, 121251 (2022).
10. M. Kusenberg *et al*., *Waste Manag.* **141**, 104–114 (2022).
11. A. Milbrandt, K. Coney, A. Badgett, G. T. Beckham, *Resour. Conserv. Recycling* **183**, 106363 (2022).
12. "Dow and Mura Technology plan to locate Europe's largest advanced recycling facility at Dow's site in Böhlen, Germany," *Cision PR Newswire*, 14 September 2022; https://www.prnewswire.com/news-releases/dow-and-mura-technology-plan-to-locate-europes-largest-advanced-recycling-facility-at-dows-site-in-bohlen-germany-301624125.html [accessed 15 October 2022].
13. J. Ma *et al*., *Green Chem.* **25**, 1032–1044 (2023).
14. B. Zhang, C. Kubis, R. Franke, *Science* **377**, 1223–1227 (2022).
15. I. Ro *et al*., *Nature* **609**, 287–292 (2022).
16. S. Lee, A. Patra, P. Christopher, D. G. Vlachos, S. Caratzoulas, *ACS Catal.* **11**, 9506–9518 (2021).
17. I. Ro, M. Xu, G. W. Graham, X. Pan, P. Christopher, *ACS Catal.* **9**, 10899–10912 (2019).
18. B. Liu *et al*., *Chem* **8**, 2630–2658 (2022).
19. A. C. Brezny, C. R. Landis, *Acc. Chem. Res.* **51**, 2344–2354 (2018).
20. D. S. Laitar, J. W. Kramer, B. T. Whiting, E. B. Lobkovsky, G. W. Coates, *Chem. Commun.* (38): 5704–5706 (2009).
21. M. Mulzer, G. W. Coates, *Org. Lett.* **13**, 1426–1428 (2011).
22. J. Yang, F. G. Delolo, A. Spannenberg, R. Jackstell, M. Beller, *Angew. Chem. Int. Ed.* **61**, e202112597 (2022).
23. F. E. Paulik, *Catal. Rev. Sci. Eng.* **6**, 49–84 (1972).
24. M. F. Mirbach, *Trans. Met. Chem.* **9**, 465–468 (1984).
25. G. W. Huber, S. Iborra, A. Corma, *Chem. Rev.* **106**, 4044–4098 (2006).
26. EIA, Petroleum & Other Liquids Spot Prices; https://www.eia.gov/dnav/pet/pet_pri_spt_s1_d.htm [accessed 2 October 2022].
27. *Plasticizer Alcohols (C4-C13) Chemical Economics Handbook* (S&P Global, 2021); https://ihsmarkit.com/products/plasticizer-alcohols-chemical-economics-handbook.html.
28. I. Mastalski *et al*., *Chem. Mater.* **35**, 3628–3639 (2023).
29. M. J. Frisch, M. Head-Gordon, J. A. Pople, *Chem. Phys. Lett.* **166**, 275–280 (1990).
30. R. Ditchfield, W. J. Hehre, J. A. Pople, *J. Chem. Phys.* **54**, 724–728 (1971).
31. G. A. Petersson *et al*., *J. Chem. Phys.* **89**, 2193–2218 (1988).
32. A. Ciroth, *Int. J. Life Cycle Assess.* **12**, 209–210 (2007).
33. C. L. Hans, K. T. Goris, D. Bien, A. E. Carpenter, C. M. Diaz, Methods for producing higher alcohols from waste plastic pyrolysis oil and the higher alcohols obtained therefrom, Patent WO2022084238A1 (2022); https://patentimages.storage.googleapis.com/a5/54/1f/25178be8451df5/WO2022084238A1.pdf.
34. R. C. DiPucchio, S.-C. Rosca, L. L. Schafer, *J. Am. Chem. Soc.* **144**, 11459–11481 (2022).
35. S. S. Scott, S.-C. Roşca, D. J. Gilmour, P. Brant, L. L. Schafer, *ACS Macro Lett.* **10**, 1266–1272 (2021).
36. P. M. Edwards, L. L. Schafer, *Org. Lett.* **19**, 5720–5723 (2017).
37. A. Tennakoon *et al*., *Nat. Catal.* **3**, 893–901 (2020).
38. G. Zichittella *et al*., *JACS Au* **2**, 2259–2268 (2022).
39. R. J. Conk *et al*., *Science* **377**, 1561–1566 (2022).
40. N. M. Wang *et al*., *J. Am. Chem. Soc.* **144**, 18526–18531 (2022).
41. S. Dong *et al*., *Appl. Catal. B* **324**, 122219 (2023).
42. T. W. Walker *et al*., *Sci. Adv.* **6**, eaba7599 (2020).
43. T. J. Fazekas *et al*., *Science* **375**, 545–550 (2022).
44. K. P. Sullivan *et al*., *Science* **378**, 207–211 (2022).
45. U. Kanbur *et al*., *Chem* **7**, 1347–1362 (2021).
46. J. Klier, J. Bohling, M. Keefe, *AIChE J.* **62**, 2238–2247 (2016).
47. L. Zheng *et al*., *ACS Sustain. Chem. Eng.* **10**, 5781–5791 (2022).
48. J. Risher, (US Department of Health and Human Services, 1995); https://stacks.cdc.gov/view/cdc/6251.
49. J. G. Speight, in *Subsea and Deepwater Oil and Gas Science and Technology* (Gulf, 2015), pp. 1–43.

ACKNOWLEDGMENTS

The authors acknowledge K. L. Vorst and G. W. Curtzweiler for providing the postconsumer colored HDPE material, mostly from personal care packaging, used for this study. The authors acknowledge H. Radhakrishnan for performing the CHN(O)S elemental analysis. H.L. thanks Y. Jiang, M. S. Kim, and J. C. Chan for helpful discussion. The authors also acknowledge J. Dumesic for providing helpful comments on the manuscript. **Funding:** This material is based on work supported by the US Department of Energy (DOE), Office of Energy Efficiency and Renewable Energy, Bioenergy Technologies Office under Award Number DEEE0009285. Z.J. and M.M. used resources at the National Energy Research Scientific Computing Center, a DOE Office of Science User Facility that is supported by the DOE, Office of Science, under contract no. DE-AC02-05CH11231 using NERSC award BES-ERCAP0022773. Part of the computational work was carried out by using supercomputing resources at the Center for Nanoscale Materials (CNM), a DOE Office of Science User Facility located at Argonne National Laboratory that is supported by DOE contract DE-AC02-06CH11357, and at the UW-Madison Center for High Throughput Computing (CHTC). CHTC is supported by UW-Madison, the Advanced Computing Initiative, the Wisconsin Alumni Research Foundation, the Wisconsin Institutes for Discovery, and the National Science Foundation. **Author contributions:** H.L. and G.W.H. designed the experiments, wrote the manuscript, and reviewed and edited the manuscript. J.W. performed pyrolysis experiments, assisted with the modeling, and reviewed and edited the manuscript. Z.J. and M.M. designed pyrolysis modeling, analyzed data, wrote modeling section, and reviewed and edited the manuscript. C.R.L. provided experimental guidance, and reviewed and edited the manuscript. H.L. and J.M. performed the technoeconomic analysis and life cycle assessment. V.M.Z. and G.W.H. provided guidance for technoeconomic analysis and life cycle assessment, and reviewed and edited the manuscript. **Competing interests:** H.L., J.W., C.R.L., and G.W.H. are inventors on US patent application P230014US01 "Method for making aldehydes, alcohols, amides, and carboxylic acids from plastic pyrolysis oil" (UW-Madison, WARF, filed 1 November 2022). G.W.H. has an ownership interest in Anellotech, which is commercializing the PlasTCat technology. **Data and materials availability:** All data are available in the main text or the supplementary materials.

SUPPLEMENTARY MATERIALS

Submitted 15 February 2023; resubmitted 12 May 2023
Accepted 15 June 2023
10.1126/science.adh1853